JOC The Journal of Organic Chemistry

Article

pubs.acs.org/joc

Tetracyclo(2,7-carbazole)s: Diatropicity and Paratropicity of Inner Regions of Nanohoops

Yasuhiro Kuroda,[†] Youichi Sakamoto,[†] Toshiyasu Suzuki,*[,†] Eiichi Kayahara,[‡] and Shigeru Yamago[‡]

[†]Institute for Molecular Science, Myodaiji, Okazaki 444-8787, Japan

[‡]Institute for Chemical Research, Kyoto University, Uji 611-0011, Japan

Supporting Information

ABSTRACT: Three N-substituted tetracyclo(2,7-carbazole)s were synthesized to investigate the inner regions of nanohoops. One compound has a 5,5-dimethylnonane bridge between two neighboring *anti*-carbazoles, which can be used as covalently bonded "methane probes". These probes near the ring center are strongly shielded by local ring currents and exhibit a singlet at δ = −2.70 ppm in ^{1}H NMR. To visualize local and macrocyclic ring currents separately, we drew nucleus-independent chemical shift contour maps of tetracyclo(9-methyl-2,7-carbazole) and [*n*]-cycloparaphenylenes (CPPs). Local ring currents make the interior diatropic, and paratropic regions exist only outside the ring. Macrocyclic ring currents in [5]CPP to [7]CPP generate deshielding cones, which are typical of antiaromatic [4*n*]annulenes.

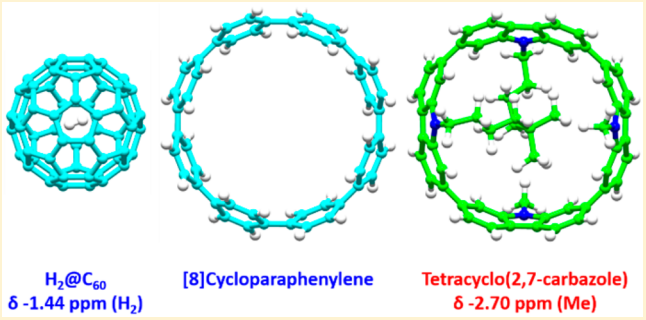

INTRODUCTION

The aromaticity of fullerenes and carbon nanotubes (CNTs) is not well understood and sometimes controversial among theorists.[1,2] Experimentally, NMR shielding provides information about the total of aromatic (diamagnetic) and antiaromatic (paramagnetic) ring currents. In the case of C_{60}, some endohedral derivatives containing atoms (He and Xe)[3,4] and small molecules (H_2 and H_2O)[5,6] have been prepared, and their NMR spectra were obtained in solution. For example, the ^{1}H NMR spectrum of H_2@C_{60} showed a singlet at δ = −1.44 ppm, which was shifted upfield by 5.98 ppm compared to free hydrogen in the same solvent.[5] [*n*]Cycloparaphenylenes (CPPs) are the shortest models for armchair (*n*,*n*) CNTs, and [5]CPP is a fragment of C_{60}.[7] The NMR shielding at the ring center would be a good indicator to see the aromaticity of CPPs because the magnetic influence of σ-bonds is the smallest. Unlike fullerenes, it is difficult to keep atoms and small molecules within CPP rings.[8] Therefore, it is necessary to design a nanohoop with covalently bonded groups near the ring center. For this purpose, we have synthesized three N-substituted tetracyclo(2,7-carbazole)s **1a**−**c**, which are derivatives of [8]CPP.[9,10] Carbazole compounds are also interesting as p-type semiconductors and thermally activated delayed fluorescent materials.[11]

RESULTS AND DISCUSSION

As shown in Scheme 1, tetracyclo(2,7-carbazole)s **1a** and **1b** were prepared by the platinum-mediated assembly method reported previously.[12,13] For comparison, model compounds **2a** and **2b** were also synthesized by the Suzuki coupling (Scheme 3). Compounds **1a** and **1b** are yellow solids and soluble in common organic solvents such as chloroform and toluene. UV−vis absorption spectra and cyclic voltammograms are shown in Figures S1 and S2. The ^{1}H and ^{13}C NMR spectra indicate that all four carbazoles are equivalent. Although the resolution is low because of the disorder of solvent molecules (toluene), the single-crystal X-ray analysis of **1a** reveals that the conformation is all-*anti* (Figure S3). Density functional theory (DFT) calculations also suggest that the all-*anti* form (Figure 1) is the most stable in four possible conformers (Figure S4). The ^{1}H NMR spectra of **1a** and **1b** (Tables S1 and S2) exhibit upfield shifts for protons within the rings compared to model compounds **2a** and **2b**, respectively (carbazole 1,8-H: $\Delta\delta$ = −1.15 ppm for **1a**, −1.08 ppm for **1b**; 9-Me in **1a**: −0.75 ppm; Ph *o*-H in **1b**: −0.56 ppm).[14,15]

To make some protons closer to the ring center, we designed a derivative with a C_9 methylene bridge between two carbazoles. At the 5-position, the C_9 chain has two methyl groups (5-Me), which can be used as covalently bonded "methane probes".[16,17] As shown in Scheme 2, we obtained *N*,*N*′-bridged tetracyclo(2,7-carbazole) **1c** that has a C_9 bridge between two neighboring carbazoles.[18] We were able to assign all aliphatic signals by COSY and HSQC (see the Supporting Information). The ^{1}H NMR spectrum exhibits a singlet at δ = −2.70 ppm for two methyl groups (5-Me), which is shifted upfield by 3.51 ppm compared to that of **3** (Table S3). The other eight protons also have negative chemical shifts at δ =

Received: February 26, 2016
Published: March 25, 2016

ACS Publications © 2016 American Chemical Society

DOI: 10.1021/acs.joc.6b00425
J. Org. Chem. 2016, 81, 3356−3363

Scheme 1. Synthesis of 1a and 1b

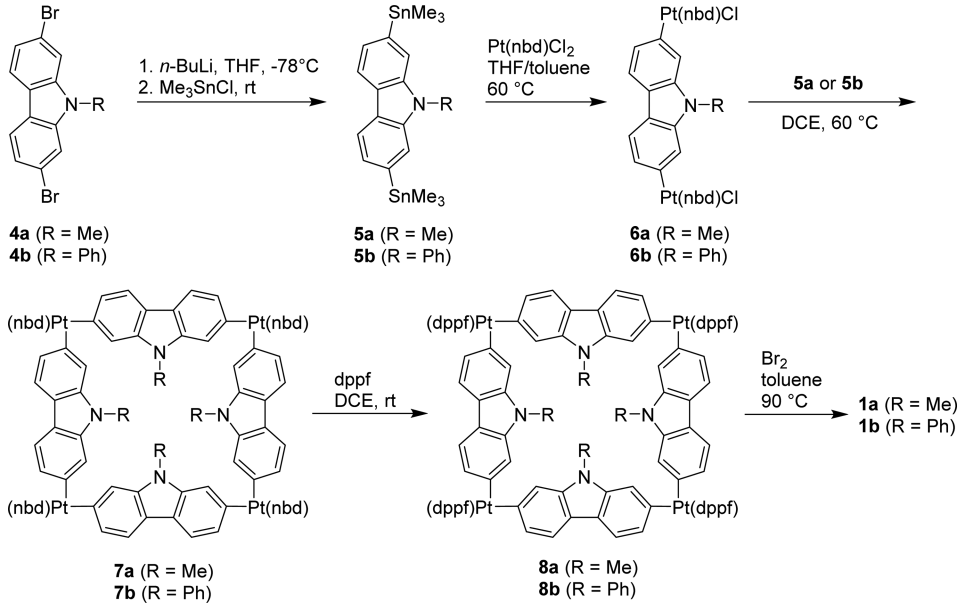

Scheme 2. Synthesis of 1c

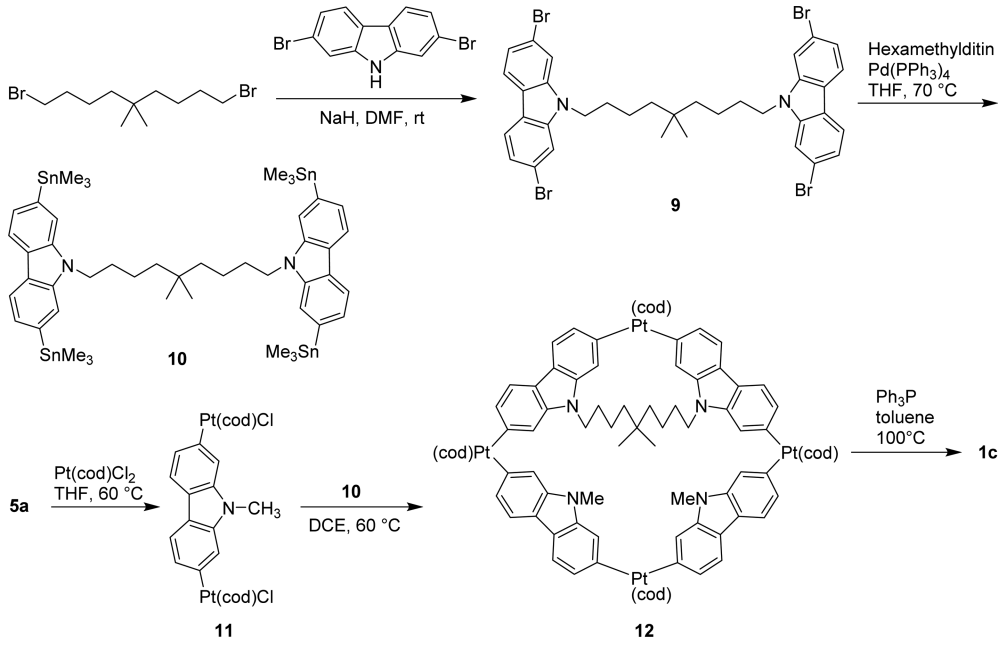

Scheme 3. Synthesis of 2a, 2b, and 3

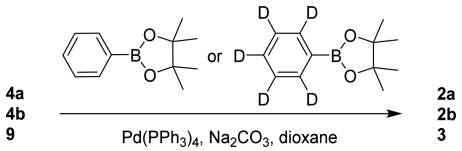

−1.49 ppm (3,7-H and 4,6-H), −1.23 ppm (3,7-H), and −1.17 ppm (4,6-H). Because only one signal was observed for two methyl groups (5-Me), we assume that the C_9 bridge is flipping rapidly at room temperature. This inversion did not freeze at −90 °C in variable-temperature ^{1}H NMR (Figure S8), indicating that the activation energy might be rather low.

The optimized geometry of **1c** (C_1 symmetry) by DFT is shown in Figure 1. Because the C_9 chain connects two *anti*-carbazoles, the C5 carbon atom with two methyl groups is located almost at the ring center. Protons 3,7-H and 4,6-H are also deep into the ring. The NMR calculation on **1c** (Table S4) supports negative chemical shifts (versus TMS) for protons 3,7-H (δ = −1.07 and −1.30 ppm), 4,6-H (−1.10 and −1.15 ppm), and 5-Me (−2.53 ppm). The activation energy for the bridge flipping is estimated to be ΔG = 5.7 kcal mol^{-1} by DFT (Figure S7), which is much lower than those for [*n*]paracyclophanes (*n* = 5 and 6: ΔG = 13−14 kcal mol^{-1} by variable-temperature ^{1}H NMR).[19] Homodesmotic reactions[20] of **1a** and **1c** indicate that bridging two carbazoles needs 11.8 kcal mol^{-1} more strain energy (Scheme S1).

To recognize the origin of the observed large upfield shifts, we examined the relationship between experimental ^{1}H NMR chemical shifts and theoretical NICS (nucleus-independent

DOI: 10.1021/acs.joc.6b00425
J. Org. Chem. 2016, 81, 3356−3363

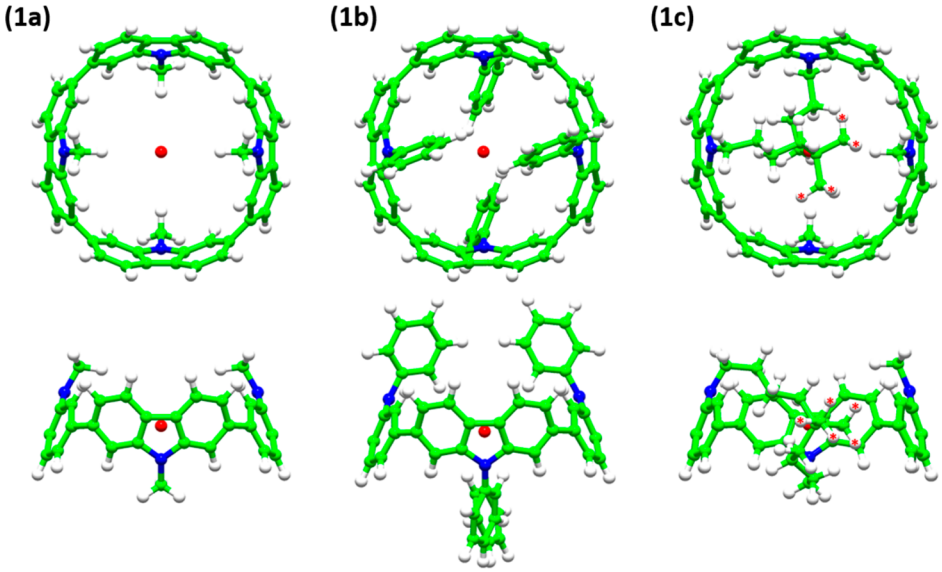

Figure 1. Optimized geometries of **1a** (D_{2d}), **1b** (D_2), and **1c** (C_1) by DFT calculations at the B3LYP/6-31G(d) level. Red circles indicate the ring centers (the mean of 48 sp^2-hybridized carbon atoms). In the side view of **1c**, the front carbazole is removed to show methane probes (red asterisks) clearly.

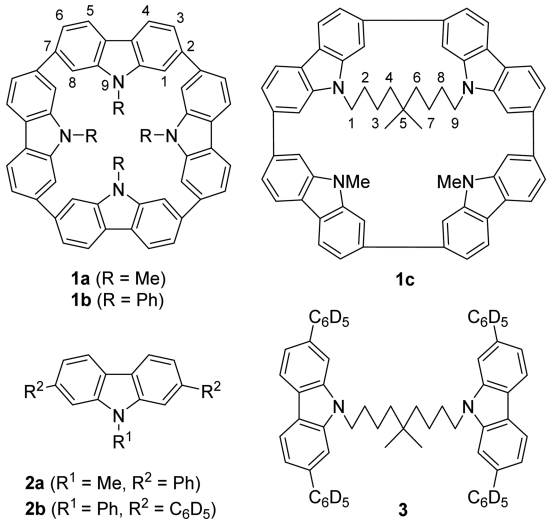

chemical shift)[21] values for [*n*]CPPs. Figure 2a shows a linear relationship (blue line) between experimental ^{1}H NMR chemical shifts and the inverse of ring radii for [8]CPP to [16]CPP.[12,22−27] From [7]CPP to [5]CPP, the deshielding effect becomes larger. Isotropic NICS ($NICS_{iso}$) values at the ring centers are also plotted against the inverse of ring radii for [*n*]CPPs (blue circles in Figure 2b). Unfortunately, this theoretical treatment did not reproduce the experimental results in Figure 2a. The apparent deshielding effect is found only for [5]CPP and not for [6]CPP and [7]CPP.

$NICS_{iso}$ is the average of three diagonal components: $NICS_{iso} = (NICS_{xx} + NICS_{yy} + NICS_{zz})/3$.[28] The $x-y$ plane corresponds to the ring plane (Figure 3a). The z axis is the same as the $C_{n/2}$ axis of [*n*]CPP when *n* is even. First, the magnetic field is applied parallel to the $x-y$ plane, which is nearly perpendicular to benzene molecular planes. This would cause diatropic ring currents by six-π-electron benzene rings (Figure 3b). Two components ($NICS_{xx} + NICS_{yy}$) should

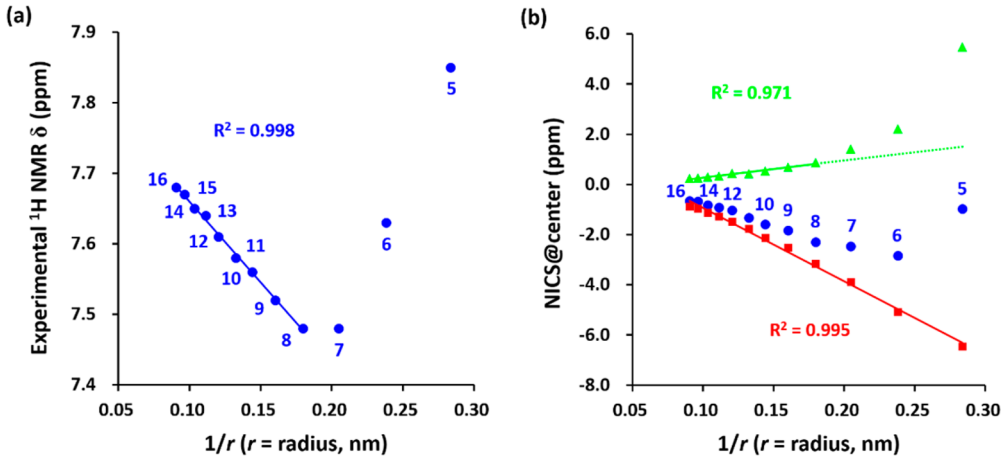

Figure 2. (a) Plot of experimental ^{1}H NMR chemical shifts versus the inverse of ring radii for [5]CPP to [16]CPP. (b) Plot of $NICS_{iso}$ (blue circles), ($NICS_{xx} + NICS_{yy}$)/3 (red squares), and $NICS_{zz}/3$ (green triangles) at the ring centers versus the inverse of ring radii for [5]CPP to [16]CPP. NICS values were obtained by the GIAO calculations at the B3LYP/6-311+G(2d,p) level.

DOI: 10.1021/acs.joc.6b00425
J. Org. Chem. 2016, 81, 3356−3363

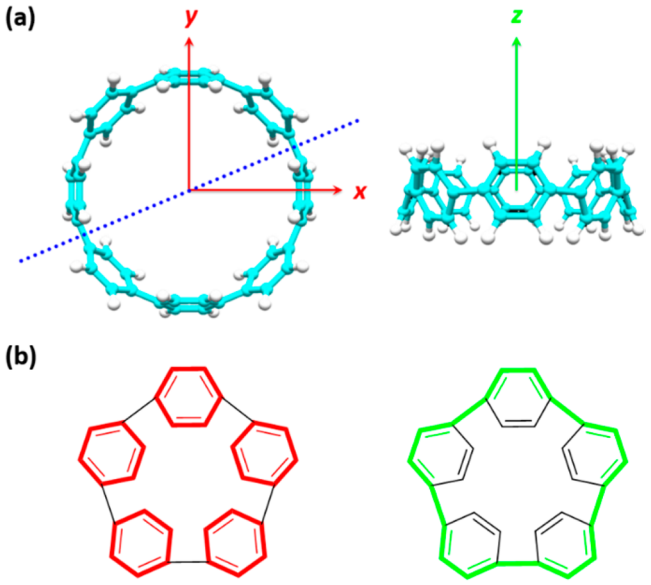

Figure 3. (a) Coordinate system for NICS calculations. A blue dotted line indicates a 2D grid for [8]CPP. (b) Local six-π-electron ring currents (diatropic) and a 20-π-electron macrocyclic ring current (paratropic) in [5]CPP.

contain this information. There is a linear relationship (a red line in Figure 2b) between $NICS_{xx}$ + $NICS_{yy}$ and the inverse of ring radii for [5]CPP to [16]CPP. A smaller [n]CPP has a more negative $NICS_{xx}$ + $NICS_{yy}$ value at the center because benzene rings are closer to the center. Second, the magnetic field is applied along the z axis, which is nearly parallel to benzene molecular planes. In the case of $NICS_{zz}$,[29] however, a similar linear relationship (a green line in Figure 2b) is found only from [8]CPP to [16]CPP. These small paramagnetic components are most likely from the σ contribution. From [7]CPP to [5]CPP, an increase of the paramagnetic component is significant. This could be attributed to a macrocyclic ring current for an antiaromatic [$4n$]annulene (Figure 3b).[30,31]

We drew NICS contour maps[32,33] to visualize local and macrocyclic ring currents separately. A two-dimensional (2D) grid (20 Å × 20 Å with a step size of 0.5 Å, 1681 points) is placed across carbon−carbon single bonds between two phenyls (dotted line in Figure 3a). Figure 4 shows contour maps of ($NICS_{xx}$ + $NICS_{yy}$)/3 for [5]CPP to [8]CPP, which visualize diamagnetic ring currents by six-π-electron benzene rings. These maps also include the σ contribution near the CPP framework.[32] The space within the ring is diatropic (red), and paratropic regions (green) exist only outside the ring. Compound **1a** also gave a contour map similar to that of [8]CPP (Figure 6). This is why the inner protons of compounds **1a**−**c** are shifted upfield.

To visualize a macrocyclic ring current in pure form, we needed to remove the influence of σ-bonds. We added two

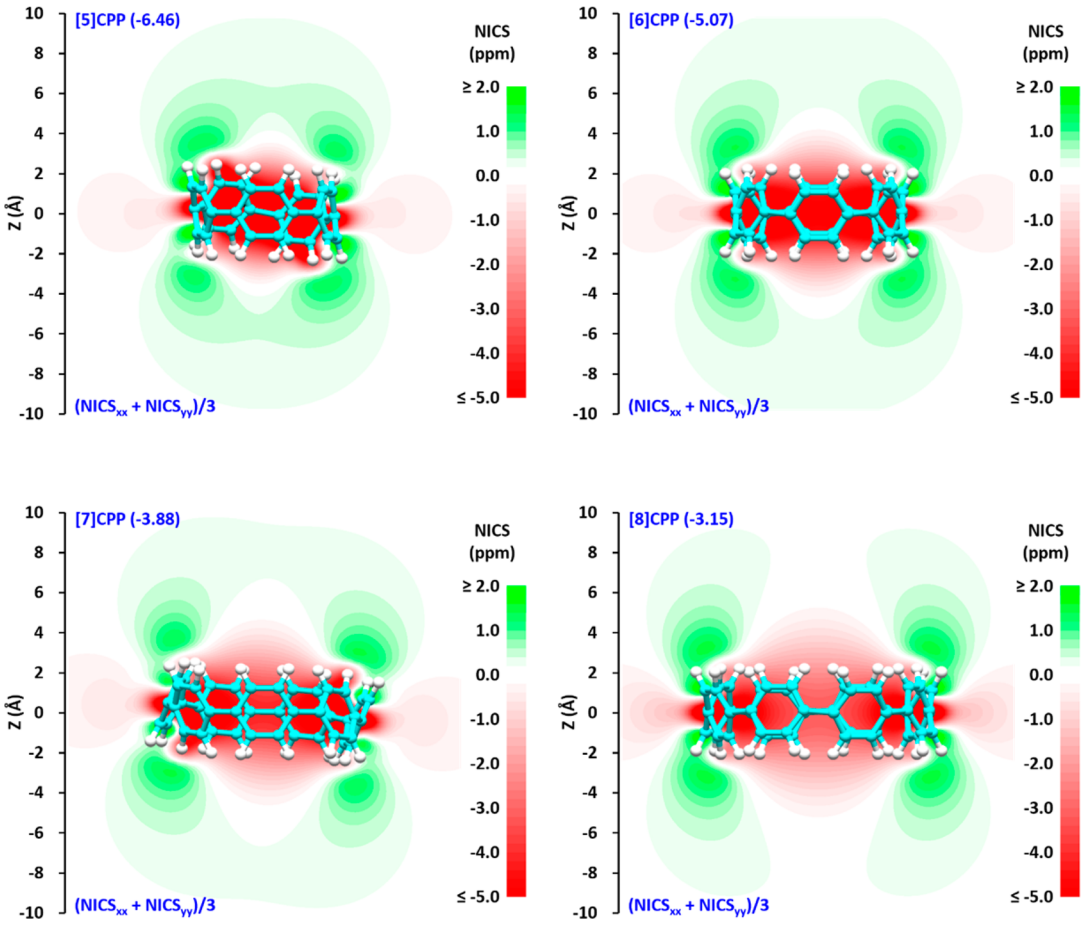

Figure 4. Contour maps of ($NICS_{xx}$ + $NICS_{yy}$)/3 for [5]CPP to [8]CPP visualize diamagnetic ring currents by six-π-electron benzene rings. Red, diatropic; green, paratropic. Corresponding NICS values at the ring centers in parentheses.

DOI: 10.1021/acs.joc.6b00425
J. Org. Chem. 2016, 81, 3356−3363

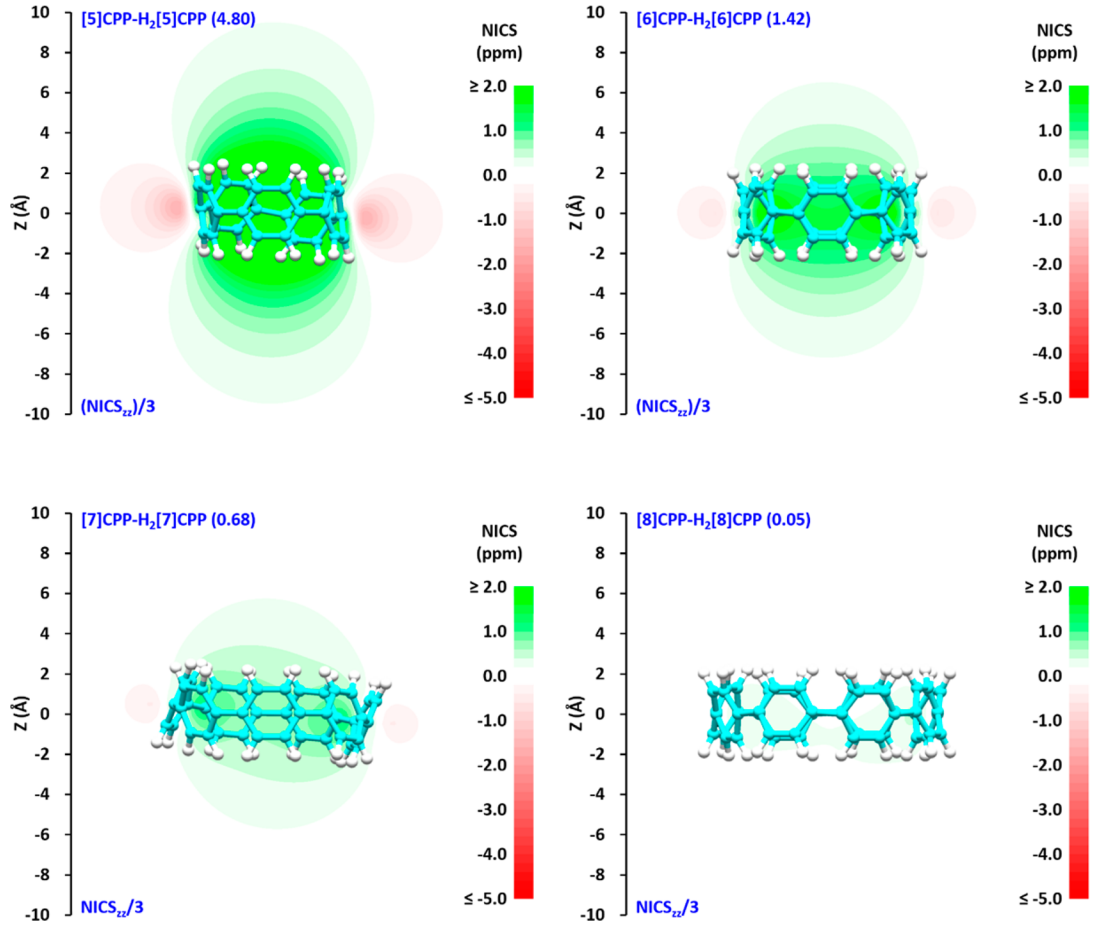

Figure 5. Contour maps of $NICS_{zz}/3([n]CPP) - NICS_{zz}/3(H_2[n]CPP)$ visualize paramagnetic ring currents by $4n$-π-electron macrocyclic rings of $[n]$CPPs. Red, diatropic; green, paratropic. Corresponding NICS values at the ring centers in parentheses.

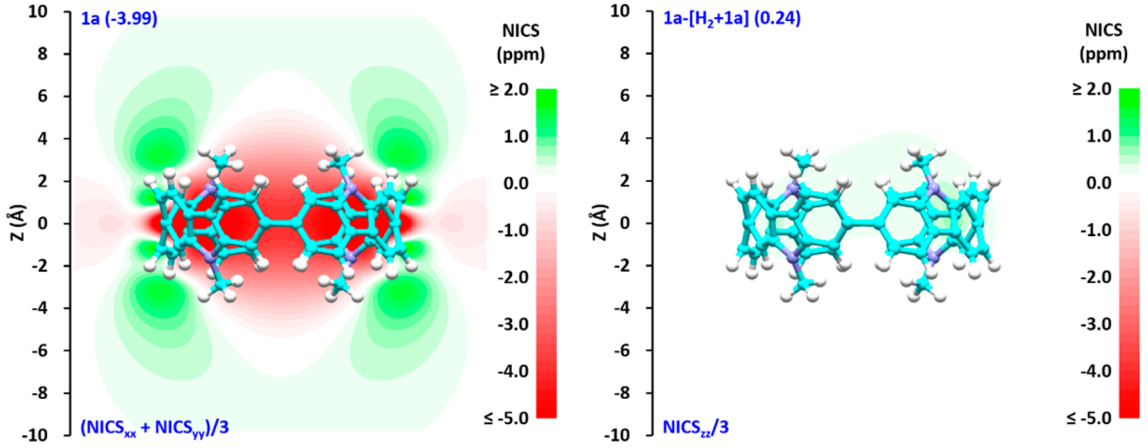

Figure 6. Contour maps of $(NICS_{xx} + NICS_{yy})/3$ for **1a** and $NICS_{zz}/3(\mathbf{1a}) - NICS_{zz}/3([H_2 + \mathbf{1a}])$. Red, diatropic; green, paratropic. Corresponding NICS values at the ring centers in parentheses.

hydrogens to the 1,4-positions of one benzene ring[34] and cut off a macrocyclic ring current (Figure S9). The resulting $H_2[n]$CPP was optimized without changing the positions of other atoms. $NICS_{zz}$ for $H_2[n]$CPP would correspond to the σ contribution. Then, it was subtracted from $NICS_{zz}$ for $[n]$CPP, which would give a pure macrocyclic ring current. A contour map of $NICS_{zz}/3([5]CPP) - NICS_{zz}/3(H_2[5]CPP)$ in Figure 5 displays a nice deshielding cone (green) of [5]CPP.[35] This is typical of antiaromatic $[4n]$annulenes such as planar D_{4h} cyclooctatetraene (Figure S10). Both [8]CPP and **1a** (Figure 6) have negligible macrocyclic ring currents.[36] The paramagnetic ring currents for [5]CPP to [7]CPP should be responsible for the deshielding effect found in Figure 2a.

Figure 7 shows isosurfaces of $NICS_{iso}$ at −0.1 ppm (red, diatropic) and 0.1 ppm (green, paratropic) for [5]CPP to [8]CPP. A three-dimensional grid of 30 Å × 30 Å × 30 Å with a step size of 0.5 Å (226,981 points) was used for NMR calculations. These isosurfaces are essentially the same as

DOI: 10.1021/acs.joc.6b00425
J. Org. Chem. 2016, 81, 3356−3363

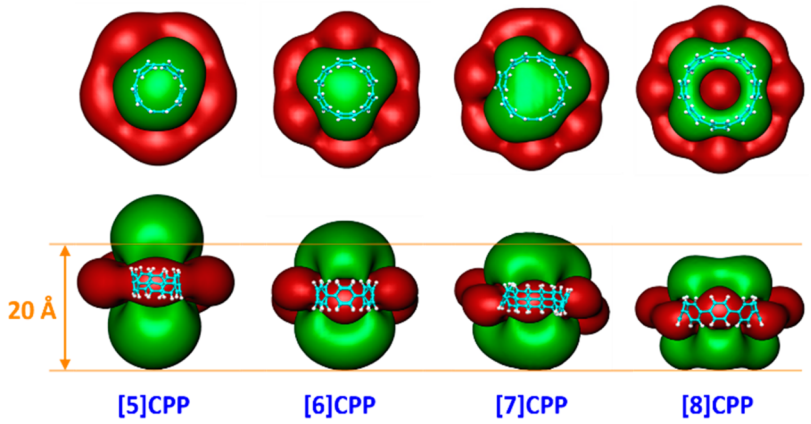

Figure 7. Isosurfaces of $NICS_{iso}$ for [5]CPP to [8]CPP from the top and the side. Red, diatropic at −0.1 ppm; green, paratropic at 0.1 ppm.

isochemical shielding surfaces (except signs and colors) developed by Kleinpeter et al.[37] Interestingly, [8]CPP and **1a** (Figure S13) have "holes" in paratropic regions because their macrocyclic ring currents are negligible. A smaller [*n*]CPP displays a taller side view, suggesting a greater paramagnetic ring current. This can be explained by an increase of the quinonoid character in a smaller [*n*]CPP.[38,39]

To understand the mechanism for the formation of a diatropic interior in [*n*]CPP, we performed a NMR calculation on benzene molecules. Eight benzene molecules are placed on a circle with a diameter of 20 Å (Figure S11). Because shielding cones of benzene molecules focus on the center, diatropic components are concentrated within the circle. Also, paratropic components of benzene molecules extend along tangent lines and exist mostly outside the circle. As a result, the inner part is diatropic, which should shield atoms and molecules. This would also be the case for [*n*]CPPs (Figure S12) and CNTs.[2,40,41]

Aihara et al. mentioned that "macrocyclic conjugation is never the main origin of global aromaticity".[42] Because the intensity of a ring current is proportional to the area of the circuit, a macrocyclic ring current often looks much larger than aromatic sextet ring currents. Therefore, even though a molecule has a strong paramagnetic ring current, it does not mean that it is globally antiaromatic. For example, some 4*n*-π-electron porphyrinoids, such as orangarin (20 π-electrons) and amethyrin (24 π-electrons),[43] show strong paramagnetic ring currents (Figure S10), but they are still stable and globally aromatic. The paramagnetic ring current of [5]CPP (20 π-electrons) is induced purely by the strain and is much smaller than that of orangarin. The question is whether [4]CPP is globally aromatic or antiaromatic. The $NICS_{iso}$ value for [4]CPP is positive (1.44) at the center, which should lead to the deshielding effect (Figures S9 and S12).

In conclusion, we have synthesized 5,5-dimethylnonane-bridged tetracyclo(2,7-carbazole) **1c**, in which two methane probes are covalently bonded and encapsulated within the ring. They are forced to stay near the ring center and are strongly shielded by local ring currents. Further study on smaller [*n*]CPPs using methane probes is currently in progress.

EXPERIMENTAL SECTION

General Experimental Methods. All reactions were carried out under an argon atmosphere. Flash chromatographic separations were performed using the Yamazen Hi-Flash column (silica gel 40 μm). Recycling preparative gel permeation chromatography was carried out using Japan Analytical Industry JAIGEL-2H and -1H. All reagents were commercially available and used as received.

9-Methyl-2,7-bis(trimethylstannyl)carbazole (5a). 2,7-Dibromo-9-methylcarbazole[44] (**4a**; 3.00 g, 8.85 mmol) was dissolved in 50 mL of dry THF and cooled to −78 °C. To this solution was added a 2.6 M solution of *n*-BuLi in hexane (8.4 mL, 21.8 mmol). After being stirred for 2 h at −78 °C, a 1.0 M solution of Me_3SnCl in THF (27.0 mL, 27.0 mmol) was added, and the mixture was stirred for 4 h. Water was added to the mixture, and the organic phase was washed with brine and dried over $MgSO_4$. After removal of the solvent, the residue was recrystallized from EtOH to afford **5a** (3.10 g, 68%) as a colorless solid: mp 123−124 °C; ^{1}H NMR (400 MHz, $CDCl_3$) δ 0.37 (s, 18H), 3.89 (s, 3H), 7.32 (d, 2H, J = 7.6 Hz), 7.51 (s, 2H), 8.07 (d, 2H, J = 8.2 Hz); ^{13}C NMR (100 MHz, $CDCl_3$) δ −9.1, 29.0, 115.5, 119.8, 123.0, 125.7, 139.4, 140.7; HRMS (FAB/quadrupole) m/z calcd for $C_{19}H_{27}NSn_2$ $[M]^+$ 507.0182, found 507.0185.

Tetracyclo(9-methyl-2,7-carbazole) (1a). A mixture of **5a** (68 mg, 0.13 mmol) and dichloro(norbornadiene)platinum(II) [Pt(nbd)-Cl_2] (100 mg, 0.28 mmol) in 2:1 dry THF/toluene (18 mL) was stirred at 60 °C for 18 h. The solvent was removed under reduced pressure. The residue was suspended in hexane followed by filtration to give **6a** as a brown solid. A suspension of **6a** (811 mg, 0.980 mmol) and **5a** (498 mg, 0.980 mmol) in 1,2-dichloroethane (400 mL) was stirred for 40 h at 60 °C. The solvent was removed under reduced pressure, and the residue was washed with hexane to give **7a** as a brown solid. To a stirred suspension of **7a** (980 mg, 0.525 mmol) in dry CH_2Cl_2 (270 mL) was added 1,1′-bis(diphenylphosphino)-ferrocene (1.07 g, 1.93 mmol) at room temperature, and the mixture was stirred for 24 h. The solvent was removed under reduced pressure, and the residue was washed with ethyl acetate to give **8a** as a brown solid. To a stirred suspension of **8a** (1.57 g, 0.423 mmol) in dry toluene (200 mL) was added Br_2 (262 mg, 1.64 mmol) at room temperature. The reaction mixture was heated to 90 °C and stirred for 12 h. The precipitate was removed by filtration. After removal of the solvent, the residue was purified by column chromatography on silica gel with 1:1 chloroform/hexane. Preparative gel permeation chromatography with chloroform gave **1a** (33 mg, 10% from **5a**) as a yellow solid: mp >370 °C; ^{1}H NMR (400 MHz, $CDCl_3$) δ 3.19 (s, 12H), 6.45 (s, 8H), 7.49 (d, 8H, J = 8.2 Hz), 7.92 (d, 8H, J = 8.2 Hz); ^{13}C NMR (100 MHz, $CDCl_3$) δ 29.4, 115.7, 116.8, 122.2, 122.4, 141.6, 144.8; HRMS (EI/quadrupole) m/z calcd for $C_{52}H_{36}N_4$ $[M]^+$ 716.2940, found 716.2947.

9-Methyl-2,7-diphenylcarbazole (2a). A 1.78 M aqueous solution of Na_2CO_3 (30 mL, 53.4 mmol) was added to a mixture of **4a** (1.00 g, 2.95 mmol), 4,4,5,5-tetramethyl-2-phenyl-1,3,2-dioxaborolane (1.20 g, 5.90 mmol), and tetrakis(triphenylphosphine)palladium (58 mg, 0.059 mmol) in dioxane (30 mL). The mixture was stirred at 100 °C overnight and extracted with hexane. The organic layer was washed with brine and dried with Na_2SO_4. After removal of the solvent, the residue was purified by chromatography on silica gel with 1:1 chloroform/hexane to afford **2a** as a colorless solid (679 mg, 69%):

DOI: 10.1021/acs.joc.6b00425
J. Org. Chem. 2016, 81, 3356−3363

mp 224−225 °C; ^{1}H NMR (400 MHz, $CDCl_3$) δ 3.94 (s, 3H), 7.37 (t, 2H, J = 7.6 Hz), 7.48 (t, 6H, J = 7.6 Hz), 7.73 (d, 4H, J = 7.6 Hz), 7.59 (s, 2H), 8.13 (d, 2H, J = 7.9 Hz); ^{13}C NMR (100 MHz, $CDCl_3$) δ 29.1, 107.1, 118.8, 120.6, 121.9, 127.1, 127.6, 128.9, 139.2, 142.1, 142.2; HRMS (EI/quadrupole) m/z calcd for $C_{25}H_{19}N$ $[M]^+$ 333.1517, found 333.1512.

9-Phenyl-2,7-bis(trimethylstannyl)carbazole (5b). 2,7-Dibromo-9-phenylcarbazole[45] (**4b**; 4.00 g, 9.97 mmol) was dissolved in 70 mL of dry THF and cooled to −78 °C. To this solution was added a 2.6 M solution of *n*-BuLi in hexane (9.6 mL, 25.0 mmol). After being stirred for 2 h at −78 °C, a 1.0 M solution of Me_3SnCl in THF (30.5 mL, 30.5 mmol) was added, and the solution was stirred for 16 h. Water was added to the solution. The organic layer was washed with brine and dried over $MgSO_4$. After removal of the solvent, the residue was recrystallized from EtOH to afford **5b** (4.01 g, 70%) as a colorless solid: mp 139−140 °C; ^{1}H NMR (400 MHz, $CDCl_3$) δ 0.29 (s,18H), 7.38 (d, 2H, J = 7.3 Hz), 7.50 (s, 2H), 7.57−7.66 (m, 5H), 8.11(d, 2H, J = 7.6 Hz); ^{13}C NMR (100 MHz, $CDCl_3$) δ −9.1, 116.7, 119.8, 123.6, 126.8, 127.2, 127.4, 129.9, 137.8, 139.9, 140.5; HRMS (FAB/quadrupole) m/z calcd for $C_{24}H_{29}NSn_2$ $[M]^+$ 569.0338, found 569.0340.

Tetracyclo(9-phenyl-2,7-carbazole) (1b). A mixture of **5b** (460 mg, 0.809 mmol) and Pt(nbd)Cl_2 (606 mg, 1.62 mmol) in 1,2-dichloroethane (120 mL) was stirred at 60 °C for 18 h. After removal of the solvent, the residue was suspended in hexane followed by filtration to give **6b** as a brown solid. A suspension of **6b** (770 mg, 0.868 mmol) and **5b** (494 mg, 0.868 mmol) in 1,2-dichloroethane (300 mL) was stirred for 40 h at 60 °C. After removal of the solvent, the residue was washed with hexane to give **7b** as a brown solid. To a stirred suspension of **7b** (1.02 g, 0.482 mmol) in dry CH_2Cl_2 (200 mL) was added 1,1′-bis(diphenylphosphino)ferrocene (1.07 g, 1.93 mmol) at room temperature, and the mixture was stirred for 24 h. After removal of the solvent, the residue was washed with ethyl acetate to give **8b** as a brown solid. To a stirred suspension of **8b** (1.12 g, 0.297 mmol) in toluene (250 mL) was added Br_2 (189 mg, 1.19 mmol) at room temperature. The reaction mixture was heated to 90 °C and stirred for 12 h. The precipitate was removed by filtration. After removal of the solvent, the residue was purified by column chromatography on silica gel with 1:1 chloroform/hexane. Preparative gel permeation chromatography with chloroform gave **1b** (78 mg, 10% from **5b**) as a yellow solid: mp >370 °C; ^{1}H NMR (400 MHz, CD_2Cl_2) δ 6.50 (s, 8H), 7.05 (d, 8H, J = 7.3 Hz), 7.34 (d, 8H, J = 8.2 Hz), 7.42 (m, 12H), 7.82 (d, 8H, J = 8.2 Hz); ^{13}C NMR (100 MHz, CD_2Cl_2) δ 116.5, 117.2, 122.2, 122.5, 127.4, 127.6, 129.8, 137.4, 141.2, 144.5; HRMS (EI/quadrupole) m/z calcd for $C_{72}H_{44}N_4$ $[M]^+$ 964.3566, found 964.3552.

4,4,5,5-Tetramethyl-2-(phenyl-d_5)-1,3,2-dioxaborolane. A 2.69 M hexane solution of *n*-BuLi (3.3 mL, 8.8 mmol) was added to a solution of bromobenzene-d_5 (1.50 g, 9.25 mmol) in dry THF (30 mL) at −80 °C. After being stirred at −80 °C for 30 min, 2-isopropoxy-4,4,5,5-tetramethyl-1,3,2-dioxaborolane (2.10 g, 11.1 mmol) was added. The reaction mixture was allowed to warm to room temperature, poured into 1 M HCl, extracted with ether, and dried with Na_2SO_4. After removal of the solvent, the residue was purified by chromatography on silica gel with hexane to afford the title compound as a colorless solid (1.08 g, 57%): ^{1}H NMR (400 MHz, $CDCl_3$) δ 1.34 (s, 12H).

2,7-Diphenyl-9-(phenyl-d_5)-9*H*-carbazole (2b). A 1.78 M aqueous solution of Na_2CO_3 (30 mL, 53.4 mmol) was added to a mixture of **4b** (1.00 g, 2.49 mmol), 4,4,5,5-tetramethyl-2-(phenyl-d_5)-1,3,2-dioxaborolane (1.04 g, 4.99 mmol), and tetrakis(triphenylphosphine)palladium (58 mg, 0.050 mmol) in dioxane (30 mL). The mixture was stirred at 100 °C overnight and extracted with hexane. The organic layer was washed with brine and dried with Na_2SO_4. After removal of the solvent, the residue was purified by chromatography on silica gel with 1:1 chloroform/hexane to afford **2b** as a colorless solid (735 mg, 40%): mp 231−232 °C; ^{1}H NMR (400 MHz, CD_2Cl_2) δ 7.50 (tt, 1H, J = 4.4 Hz, 4.4 Hz), 7.55 (d, 2H, J = 8.2 Hz), 7.60 (s, 2H), 7.63 (d, 4H, J = 4.4 Hz), 8.19 (d, 2H, J = 8.2 Hz); ^{13}C NMR (100 MHz, CD_2Cl_2) δ 108.2, 119.7, 120.6, 122.3, 126.4, 126.6, 126.7, 126.9, 127.0, 127.2, 127.3, 127.7, 128.0, 128.2, 128.5, 130.1, 137.5, 139.4, 141.6, 142.1; HRMS (EI/quadrupole) m/z calcd for $C_{30}H_{11}D_{10}N$ $[M]^+$ 405.2302, found 405.2288.

9,9′-(5,5-Dimethylnonane-1,9-diyl)bis(2,7-dibromocarbazole) (9). A mixture of 2,7-dibromocarbazole (1.00 g, 3.07 mmol), 60% NaH (171 mg, 4.3 mmol), and dry DMF (20 mL) was stirred at room temperature. After being stirred for 30 min, 1,9-dibromo-5,5-dimethylnonane[46] (481 mg, 1.53 mmol) was added, and the solution was stirred for 18 h. The reaction mixture was poured into water and extracted with CH_2Cl_2. The organic layer was washed with brine and dried with $MgSO_4$. After removal of the solvent, the residue was recrystallized from ethyl acetate to give **9** (620 mg, 50%): mp 153−154 °C; ^{1}H NMR (400 MHz, $CDCl_3$) δ 0.80 (s, 6H), 1.17 (m, 4H), 1.21 (m, 4H), 1.71 (m, 4H), 4.01 (t, 4H, J = 7.2 Hz) 7.28 (d, 4H, J = 8.0 Hz), 7.46 (s, 4H), 7.77 (d, 4H, J = 8.0 Hz); ^{13}C NMR (100 MHz, $CDCl_3$) δ 21.6, 27.2, 29.4, 32.7, 41.3, 43.1, 112.0, 119.7, 121.3, 121.5, 122.6, 141.3; HRMS (EI/quadrupole) m/z calcd for $C_{35}H_{34}Br_4N_2$ $[M]^+$ 801.9415, found 801.9406.

9,9′-(5,5-Dimethylnonane-1,9-diyl)bis(2,7-bis(trimethylstannyl)carbazole) (10). Hexamethylditin (821 mg, 2.52 mmol) and **9** (340 mg, 0.42 mmol) were added to tetrakis(triphenylphosphine)palladium (60 mg, 51 μmol) in dry THF (10 mL). The mixture was stirred at 70 °C overnight and extracted with CH_2Cl_2. The organic layer was washed with brine and dried with Na_2SO_4. After removal of the solvent, the residue was purified by preparative gel permeation chromatography with chloroform to give **10** as a colorless solid (320 mg, 67%): mp 73−74 °C; ^{1}H NMR (600 MHz, $CDCl_3$) δ 0.35 (s, 36H), 0.77 (s, 6H), 1.23 (m, 4H), 1.30 (m, 4H), 1.83 (m, 4H), 4.30 (t, 4H, J = 7.2 Hz), 7.31 (d, 4H, J = 7.2 Hz), 7.51 (s, 4H), 8.07 (d, 4H, J = 7.2 Hz); ^{13}C NMR (150 MHz, $CDCl_3$) δ −9.0, 22.1, 26.9, 30.0, 32.7, 42.0, 42.8, 115.8, 119.9, 123.1, 125.6, 139.1, 140.0.

1c. A mixture of **5a** (1.00 g, 1.97 mmol) and dichloro(1,5-cyclooctadiene)platinum(II) [Pt(cod)Cl_2] (1.50 g, 4.00 mmol) in dry THF (400 mL) was stirred at 60 °C for 18 h. After removal of the solvent, the residue was suspended in hexane followed by filtration to give **11** as a brown solid. A suspension of **11** (300 mg, 0.350 mmol) and **10** (200 mg, 0.176 mmol) in 1,2-dichloroethane (600 mL) was stirred for 40 h at 60 °C. After removal of the solvent, the residue was washed with hexane to give **12** as a brown solid. A suspension of **12** (350 mg, 0.170 mmol) and triphenylphosphine (444 mg, 1.69 mmol) in dry toluene (30 mL) was stirred for 24 h at 100 °C. The precipitate was removed by filtration. After removal of the solvent, the residue was purified by column chromatography on silica gel with 1:1 ethyl acetate/hexane to give **1c** (15 mg, 10% from **10**) as a yellow solid: mp >370 °C; ^{1}H NMR (600 MHz, $CDCl_3$) δ −2.70 (s, 6H), −1.49 (m, 4H), −1.23 (m, 2H), −1.17 (m, 2H), 0.99 (m, 4H), 3.27 (s, 6H), 4.03 (m, 4H), 6.53 (s, 2H), 6.56 (s, 2H), 6.58 (s, 4H), 7.50 (m, 8H), 7.89 (m, 8H); ^{13}C NMR (150 MHz, $CDCl_3$) δ 18.39, 25.84, 28.15, 29.32, 29.87, 37.15, 41.89, 115.21, 115.48, 116.17, 116.20, 116.65, 116.81, 116.88, 118.01, 121.78, 122.02, 122.29, 122.32, 122.37, 122.42, 122.48, 122.51, 140.74, 140.93, 141.25, 141.55 144.07, 144.26, 145.12, 145.15; HRMS (EI/quadrupole) m/z calcd for $C_{61}H_{52}N_4$ $[M]^+$ 840.4192, found 840.4196.

9,9′-(5,5-Dimethylnonane-1,9-diyl)bis(2,7-bis(phenyl-d_5)-carbazole) (3). A 1.78 M aqueous solution of Na_2CO_3 (10 mL, 17.8 mmol) was added to a mixture of **9** (100 mg, 0.125 mmol), 4,4,5,5-tetramethyl-2-(phenyl-d_5)-1,3,2-dioxaborolane (104 mg, 0.510 mmol), and tetrakis(triphenylphosphine)palladium (10 mg, 8.6 μmol) in dioxane (10 mL). The mixture was stirred at 100 °C overnight and extracted with hexane. The organic layer was washed with brine and dried with Na_2SO_4. After removal of the solvent, the residue was purified by chromatography on silica gel with 1:1 chloroform/hexane to afford **3** as a colorless solid (90 mg, 90%): mp 194−195 °C; ^{1}H NMR (400 MHz, $CDCl_3$) δ 0.81 (s, 6H), 1.19 (m, 4H), 1.32 (m, 4H), 1.83 (m, 4H), 4.24 (t, 4H, J = 6.8 Hz), 7.45 (d, 4H, J = 8.0 Hz), 7.56 (s, 4H), 8.07 (d, 4H, J = 8.0 Hz); ^{13}C NMR (100 MHz, $CDCl_3$) δ 22.0, 27.3, 29.7, 32.7, 41.5, 43.0, 107.3, 118.8, 120.7, 122.0, 126.4, 126.6, 126.8, 127.0, 127.2, 127.5, 128.1, 128.4, 128.6, 139.1, 141.5,

DOI: 10.1021/acs.joc.6b00425
J. Org. Chem. 2016, 81, 3356−3363

142.1; HRMS (EI/quadrupole) m/z calcd for $C_{59}H_{34}D_{20}N_2$ $[M]^+$ 810.5542, found 810.5532.

■ ASSOCIATED CONTENT

Supporting Information

The Supporting Information is available free of charge on the ACS Publications website at DOI: 10.1021/acs.joc.6b00425.

Crystallographic data for **1a** (CIF)

UV−vis absorption and fluorescence, cyclic voltammograms, NICS contour maps and isosurfaces, computational details, energies and coordinates for the calculated compounds, ^{1}H and ^{13}C NMR, COSY, HSQC, and HMQC (PDF)

■ AUTHOR INFORMATION

Corresponding Author

*E-mail: toshy@ims.ac.jp.

Notes

The authors declare no competing financial interest.

■ ACKNOWLEDGMENTS

This work was supported by CREST, JST, and the Collaborative Research Program of Institute for Chemical Research, Kyoto University (Grant #2015-92). The computations were performed using the Research Center for Computational Science, Okazaki, Japan. Single-crystal X-ray analysis was carried out at BL02B1 of SPring-8 with the approval of the Japan Synchrotron Radiation Research Institute (JASRI; 2014B1203). We thank Dr. Kunihisa Sugimoto and Dr. Nobuhiro Yasuda (JASRI) for their valuable discussions and suggestions regarding X-ray crystallographic analysis.

■ REFERENCES

(1) Chen, Z.; Wu, J. I.; Corminboeuf, C.; Bohmann, J.; Lu, X.; Hirsch, A.; Schleyer, P. *Phys. Chem. Chem. Phys.* **2012**, *14*, 14886.

(2) Ren, P.; Zheng, A.; Xiao, J.; Pan, X.; Bao, X. *Chem. Sci.* **2015**, *6*, 902.

(3) Saunders, M.; Jimenezvazquez, H. A.; Cross, R. J.; Mroczkowski, S.; Freedberg, D. I.; Anet, F. A. L. *Nature* **1994**, *367*, 256.

(4) Syamala, M. S.; Cross, R. J.; Saunders, M. *J. Am. Chem. Soc.* **2002**, *124*, 6216.

(5) Komatsu, K.; Murata, M.; Murata, Y. *Science* **2005**, *307*, 238.

(6) Kurotobi, K.; Murata, Y. *Science* **2011**, *333*, 613.

(7) Lewis, S. E. *Chem. Soc. Rev.* **2015**, *44*, 2221.

(8) Iwamoto, T.; Watanabe, Y.; Sadahiro, T.; Haino, T.; Yamago, S. *Angew. Chem., Int. Ed.* **2011**, *50*, 8342.

(9) Mysliwiec, D.; Kondratowicz, M.; Lis, T.; Chmielewski, P. J.; Stepien, M. *J. Am. Chem. Soc.* **2015**, *137*, 1643.

(10) Jung, S. H.; Pisula, W.; Rouhanipour, A.; Rader, H. J.; Jacob, J.; Mullen, K. *Angew. Chem., Int. Ed.* **2006**, *45*, 4685.

(11) Uoyama, H.; Goushi, K.; Shizu, K.; Nomura, H.; Adachi, C. *Nature* **2012**, *492*, 234.

(12) Iwamoto, T.; Watanabe, Y.; Sakamoto, Y.; Suzuki, T.; Yamago, S. *J. Am. Chem. Soc.* **2011**, *133*, 8354.

(13) Kayahara, E.; Qu, R.; Kojima, M.; Iwamoto, T.; Suzuki, T.; Yamago, S. *Chem. - Eur. J.* **2015**, *21*, 18939.

(14) A change of hybridization of carbon atoms due to nonplanarity should also be considered for carbazole 1,8-protons.

(15) Yagi, A.; Segawa, Y.; Itami, K. *J. Am. Chem. Soc.* **2012**, *134*, 2962.

(16) Martin, N. H.; Brown, J. D.; Nance, K. H.; Schaefer, H. F.; Schleyer, P. V.; Wang, Z. X.; Woodcock, H. L. *Org. Lett.* **2001**, *3*, 3823.

(17) Williams, R. V.; Armantrout, J. R.; Twamley, B.; Mitchell, R. H.; Ward, T. R.; Bandyopadhyay, S. *J. Am. Chem. Soc.* **2002**, *124*, 13495.

(18) We did not find an isomer that has a bridge between two opposite carbazoles. See Figure S5.

(19) Ernst, L. *Prog. Nucl. Magn. Reson. Spectrosc.* **2000**, *37*, 47.

(20) Segawa, Y.; Omachi, H.; Itami, K. *Org. Lett.* **2010**, *12*, 2262.

(21) Chen, Z.; Wannere, C. S.; Corminboeuf, C.; Puchta, R.; Schleyer, P. v. R. *Chem. Rev.* **2005**, *105*, 3842.

(22) Kayahara, E.; Patel, V. K.; Yamago, S. *J. Am. Chem. Soc.* **2014**, *136*, 2284.

(23) Evans, P. J.; Darzi, E. R.; Jasti, R. *Nat. Chem.* **2014**, *6*, 404.

(24) Xia, J.; Jasti, R. *Angew. Chem., Int. Ed.* **2012**, *51*, 2474.

(25) Sisto, T. J.; Golder, M. R.; Hirst, E. S.; Jasti, R. *J. Am. Chem. Soc.* **2011**, *133*, 15800.

(26) Jasti, R.; Bhattacharjee, J.; Neaton, J. B.; Bertozzi, C. R. *J. Am. Chem. Soc.* **2008**, *130*, 17646.

(27) Omachi, H.; Matsuura, S.; Segawa, Y.; Itami, K. *Angew. Chem., Int. Ed.* **2010**, *49*, 10202.

(28) Corminboeuf, C.; Heine, T.; Seifert, G.; Schleyer, P. v. R.; Weber, J. *Phys. Chem. Chem. Phys.* **2004**, *6*, 273.

(29) Gershoni-Poranne, R.; Stanger, A. *Chem. - Eur. J.* **2014**, *20*, 5673.

(30) Taubert, S.; Sundholm, D.; Pichierri, F. *J. Org. Chem.* **2010**, *75*, 5867.

(31) Toriumi, N.; Muranaka, A.; Kayahara, E.; Yamago, S.; Uchiyama, M. *J. Am. Chem. Soc.* **2015**, *137*, 82.

(32) Schleyer, P. v. R.; Manoharan, M.; Wang, Z. X.; Kiran, B.; Jiao, H. J.; Puchta, R.; van Eikema Hommes, N. J. R. *Org. Lett.* **2001**, *3*, 2465.

(33) Kleinpeter, E.; Klod, S.; Koch, A. *J. Mol. Struct.: THEOCHEM* **2007**, *811*, 45.

(34) Stanger, A. *J. Org. Chem.* **2010**, *75*, 2281.

(35) A contour map of $NICS_{iso}$([5]CPP) − $NICS_{iso}$(H_2[5]CPP) also shows a similar deshielding cone. See Figure S9.

(36) In contrast to neutral molecules, dicationic and dianionic forms are expected to have large diatropic ring currents. See Figure S9 ([8]CPP^{2+} and [8]CPP^{2-}) and refs 30 and 31. For the dication and dianion of **1c**, the chemical shifts of 5-Me are estimated to be −14.0 and −11.7 ppm, respectively, by DFT calculations at the B3LYP/6-311+G(2d,p)//B3LYP/6-31+G(d) level.

(37) Kleinpeter, E.; Krüger, S.; Koch, A. *J. Phys. Chem. A* **2015**, *119*, 4268.

(38) Fujitsuka, M.; Iwamoto, T.; Kayahara, E.; Yamago, S.; Majima, T. *ChemPhysChem* **2013**, *14*, 1570.

(39) Alvarez, M. P.; Burrezo, P. M.; Kertesz, M.; Iwamoto, T.; Yamago, S.; Xia, J. L.; Jasti, R.; Navarrete, J. T. L.; Taravillo, M.; Baonza, V. G.; Casado, J. *Angew. Chem., Int. Ed.* **2014**, *53*, 7033.

(40) Sebastiani, D.; Kudin, K. N. *ACS Nano* **2008**, *2*, 661.

(41) Kibalchenko, M.; Payne, M. C.; Yates, J. R. *ACS Nano* **2011**, *5*, 537.

(42) Nakagami, Y.; Sekine, R.; Aihara, J. *Org. Biomol. Chem.* **2012**, *10*, 5219.

(43) Sessler, J. L.; Weghorn, S. J.; Hiseada, Y.; Lynch, V. *Chem. - Eur. J.* **1995**, *1*, 56.

(44) Aristizabal, J. A.; Soto, J. P.; Ballesteros, L.; Muñoz, E.; Ahumada, J. C. *Polym. Bull.* **2013**, *70*, 35.

(45) Jiang, W.; Duan, L.; Qiao, J.; Dong, G.; Zhang, D.; Wang, L.; Qiu, Y. *J. Mater. Chem.* **2011**, *21*, 4918.

(46) Friedman, P.; Allen, P. *J. Org. Chem.* **1965**, *30*, 780.

DOI: 10.1021/acs.joc.6b00425
J. Org. Chem. 2016, 81, 3356−3363